

PHYLOGENETIC RELATIONSHIPS OF THE MARSUPIAL GENUS *HYLADELPHYS* BASED ON NUCLEAR GENE SEQUENCES AND MORPHOLOGY

SHARON A. JANSA* AND ROBERT S. VOSS

Bell Museum of Natural History and Department of Ecology, Evolution and Behavior,
University of Minnesota, St. Paul, MN 55108, USA (SAJ)

American Museum of Natural History, Central Park West at 79th Street, New York, NY 10024, USA (RSV)

Phylogenetic analyses of sequence data from the nuclear gene encoding the interphotoreceptor retinoid-binding protein (*Irbp*) provide compelling evidence that the recently described Amazonian marsupial genus *Hyladelphys* is a didelphid and suggest that it occupies an internal branch separating the traditionally recognized subfamilies Caluromyinae and Didelphinae. Although this phylogenetic position also is supported by morphological character data, analyses of sequence data from the dentin matrix protein 1 gene (*Dmp1*) place *Hyladelphys* within the didelphine radiation. A parsimony analysis of the combined morphological and molecular data supports the *Irbp*-only results, but a partitioned Bayesian analysis of the combined gene data does not provide strong support for either placement. The implications of these results are discussed in terms of long-branch attraction, base-compositional bias, and other possibly confounding factors. Whether *Hyladelphys* is the sister group of Didelphinae or an independent lineage at some basal level within that subfamily, the absence of any close relationship to other Recent taxa is clearly indicated. We redescribe the genus based on new morphological character data and comment on the probable existence of undescribed taxa in addition to *H. kalinowskii*, the type species.

Key words: Didelphidae, *Dmp1*, *Hyladelphys*, *Irbp*, Marsupialia, morphology, nuclear genes, phylogeny, systematics

In 1992 the late Philip Hershkovitz named *Gracilinanus kalinowskii* based on 2 specimens collected many years earlier in the lowland rain forests of eastern Peru. Although Hershkovitz noted that his material (consisting of traditional skin-and-skull preparations) differed in several morphological respects from Gardner and Creighton's (1989) original diagnosis of the didelphid marsupial genus *Gracilinanus*, he apparently believed that no higher-taxonomic distinction was necessary. However, subsequent study of new, anatomically complete specimens showed that *kalinowskii* is strikingly unlike any other known New World marsupial. In the absence of phylogenetically defensible combinations of the specific epithet with existing generic names, Voss et al. (2001) proposed the new genus *Hyladelphys* with *H. kalinowskii* (Hershkovitz, 1992) as its type and only recognized species. Despite additional specimens recently reported from widely scattered localities in Brazil (de Moraes, in press), French Guiana (F. Catzeflis, pers. comm.), and Peru (Hice 2001; Solari et al. 2001),

Hyladelphys is still known from fewer than a dozen individuals, and many aspects of its biology are completely unknown.

Among other enigmas, it is unclear whether or not *Hyladelphys* is really a didelphid. The essential problem consists of the absence of compelling morphological synapomorphies that support didelphid monophyly; instead, the family has traditionally been diagnosed on the basis of shared primitive characters and biogeography (Jansa and Voss 2000; Voss et al. 2001). Although side-by-side epididymal sperm-pairing is an unambiguously derived trait shared by all didelphids whose male gametes have been examined by electron microscopy (Temple-Smith 1987), special histological preparations are required for scoring this character, which remains undetermined for most Recent marsupials (including *Hyladelphys*) and—of course—all fossils. As a practical criterion for taxon recognition, therefore, sperm-pairing is of limited value.

Unfortunately, the phylogenetic significance of other potentially diagnostic morphological characters remains effectively untested. For example, all didelphids are said to have odd-numbered mammary complements because of the presence of an unpaired median teat, whereas most nondidelphid marsupials (and placental mammals) have even-numbered mammary counts because all of their teats are normally paired (Bresslau 1920; Thomas 1888; Voss et al. 2001). However, the possession

* Correspondent: jansa003@umn.edu

of odd- versus even-numbered mammary complements has yet to be scored for any morphological analysis of marsupial relationships, so it is not known whether this character alone would be sufficient to support didelphid monophyly. To date, most morphological phylogenies that have included both Old World polyprotodonts and multiple didelphid exemplars have failed to support didelphid monophyly (e.g., Kirsch and Archer 1982; Wroe et al. 2000).

As described and illustrated by Voss et al. (2001), *Hyladelphys* differs from all known didelphids by lacking an unpaired median nipple, and by having vestigial deciduous premolars (dP3/dp3). Although the former trait might be primitive and does not rule out the possibility that *Hyladelphys* is more closely related to didelphids than to other metatherian groups, the latter is plausibly interpreted as derived (Archer 1976; Lockett and Hong 2000) and provides evidence for a possibly closer relationship with paucituberculate, peramelemorph, or dasyuromorph lineages that have similarly reduced milk teeth. Given the currently inadequate morphological basis for polyprotodont clade recognition, none of these possibilities can be rejected out of hand.

By contrast with morphological analyses of marsupial relationships, some molecular studies have provided compelling support for didelphid monophyly (e.g., Jansa and Voss 2000; Kirsch et al. 1997). Among the variety of data that have been analyzed in this context, DNA sequences from the nuclear gene encoding the interphotoreceptor retinoid-binding protein (*Irbp*) offer the best prospect for resolving the phylogenetic status of *Hyladelphys*. As demonstrated by numerous recent phylogenetic studies (e.g., Jansa and Voss 2000; Jansa and Weksler 2004; Krajewski et al. 2004; Springer et al. 1997; Stanhope et al. 1996; Voss and Jansa 2003; Weksler 2003), *Irbp* nucleotide sequences provide a wealth of characters that are parsimony-informative about mammalian relationships at a variety of taxonomic levels. Didelphid monophyly, in particular, is impressively supported by 10 uniquely derived and unreversed transformations at widely scattered sites along a fragment about 1,200 base pairs (bp) long, including changes at all 3 codon positions, transitions and transversions, and mutations with both silent and replacement effects (Jansa and Voss 2000:63, table IV).

To date, *Hyladelphys* has not been included in any morphological or molecular analysis of marsupial phylogeny and its relationships are effectively unknown. However, recently collected tissues and fresh morphological material now provide an adequate basis for a meaningful synthesis of genetic and phenotypic character data. In this report, we analyze *Irbp* sequence data from 61 terminal taxa including 2 individuals of *Hyladelphys*, didelphimorphs, exemplars from 5 other marsupial orders, and 11 placental outgroups. Additional data from the nuclear gene encoding dentin matrix protein 1 (*Dmp1*) and from morphology are analyzed separately and in combination with *Irbp* to provide additional insights based on all of the information currently at hand.

MATERIALS AND METHODS

Molecular sequence data.—We obtained *Irbp* sequences from 2 ethanol-preserved tissue samples of *H. kalinowskii*. The 1st (tissue

sample number TK73757) is from a juvenile female collected by Christine L. Hice on 20 May 1998 at the Estación Biológica Alpuhuayo, approximately 25 km southwest of Iquitos in the Peruvian department of Loreto; the morphological voucher specimen for this sample (currently designated by field number CLH 2470) will eventually be cataloged in the Museum of Texas Tech University in Lubbock, Texas (C. L. Hice, pers. comm.). The 2nd tissue sample (T4385), also from a juvenile female, was collected by Mael DeWinter in December 2002 on the Route de Kaw, approximately 30 km southeast of Cayenne, French Guiana; the morphological voucher for this sample (currently designated by field number V-1791) will eventually be cataloged in the Muséum National d'Histoire Naturelle in Paris, France (F. Catzeflis, pers. comm.). Both voucher specimens were examined by the 2nd author to confirm identifications.

Our procedures for *Irbp* sequencing and alignment were described in detail by Jansa and Voss (2000) but merit summary repetition. Briefly, a region approximately 1,200 bp long of exon 1 was amplified from genomic DNA by using primers A and D1. This product was used as a template in 2 subsequent polymerase chain reactions (PCRs), 1 using primer A paired with F and 1 using primers E1 and D1. The resulting PCR product was sequenced in both directions by using amplification primers and dye terminator chemistry (BigDye Cycle Sequencing, Applied Biosystems Inc., Foster City, California). Both of the *Irbp* sequences that we obtained from *Hyladelphys* have been deposited in GenBank with accession numbers DQ112324 and DQ112325.

To assess the relationships of *Hyladelphys* with other marsupials, we analyzed *Irbp* sequence data from 42 didelphid species representing all but 1 of the currently recognized Recent genera in the order Didelphimorphia (only *Chacodelphys*, recently described by Voss et al. [2004], is not represented). As previously reported, these sequences have been deposited in Genbank with accession numbers AF257675–AF247710 (from Jansa and Voss 2000), AY233765–AY233791 (from Voss and Jansa 2003), and AY957486–AY957494 (from Voss et al. 2005). We also analyzed nondidelphid marsupial *Irbp* sequences obtained by Springer et al. (1997) representing the following higher taxa: Dasyuromorphia (*Phascogale tapoatafa* [AF025382]), Diprotodontia (*Pseudochirops cupreus* [AF025387] and *Vombatus ursinus* [AF025386]), Microbiotheria (*Dromiciops gliroides* [AF025384]), Paucituberculata (*Caenolestes fuliginosus* [AF025381]), and Peramelemorphia (*Echymipera kalubu* [AF025383]). Outgroup (nonmarsupial) *Irbp* sequences that we included to root our analyses represent the following placental clades: Artiodactyla (*Sus scrofa* [U48588]), Carnivora (*Felis catus* [Z11811]), Chiroptera (*Macrotus californicus* [U48585]), Hyracoidea (*Procavia capensis* [U8586]), Insectivora (*Erinaceus europaeus* [AF025390] and *Sorex palustris* [U48587]), Primates (*Homo sapiens* [J05253]), Proboscidea (*Loxodonta africana* [U48711]), Rodentia (*Mus musculus* [AF126968]), and Tubulidentata (*Orycteropus afer* [U48712]).

Sequences from *Dmp1* exon 6 were obtained from the same 2 tissue samples of *Hyladelphys* described above by using methods previously explained by Jansa et al. (in press). Briefly, a fragment of about 1,200 bp was amplified from genomic DNA by using primers DEN-12 and DEN-2 (Toyosawa et al. 1999). This product was used as a template in 2 subsequent PCRs, 1 using DEN-12 paired with DEN-13 and the other using DEN-2 paired with DEN-14. The resulting products were sequenced in both directions by using amplification primers and dye terminator chemistry (BigDye Cycle Sequencing, Applied Biosystems Inc.). The *Dmp1* sequences we obtained from *Hyladelphys* have been deposited in GenBank with accession numbers DQ112326 and DQ112327. *Dmp1* sequences from 41 didelphid species previously analyzed by Jansa et al. (in press) have GenBank accession numbers

DQ083120–DQ083160. The latter represent the same terminal taxa sequenced for *Irbp*, with the exception of *Caluromysiops irrupta* (from which no tissues were available for *Dmp1* amplification); the tissue samples from which these sequences were obtained are listed in Jansa and Voss (2000:appendix), Voss and Jansa (2003:appendix 2), and Voss et al. (2005:appendix 2).

Nonmolecular character data.—We scored the morphological characters described by Voss and Jansa (2003) from 8 specimens of *H. kalinowskii*, including 3 from French Guiana (AMNH [American Museum of Natural History, New York] 267003, AMNH 267338, AMNH 267339, and V-1791 [the morphological voucher of the 2nd tissue sample described above]), 3 from Peru (FMNH [Field Museum of Natural History, Chicago, Illinois] 65754, FMNH 89991, and MUSM [Museo de Historia Natural de la Universidad Nacional Mayor de San Marcos, Lima, Peru] 11031), and 1 from Guyana (ROM [Royal Ontario Museum, Toronto, Ontario, Canada] 34271). With the exception of V-1791, in-country locality data from all of these specimens were summarized by Voss et al. (2001). Although we did not examine the Brazilian specimen of *H. kalinowskii* reported by de Moraes (in press), digital images and verbal descriptions provided by the author (pers. comm.) usefully supplemented our firsthand morphological observations from the other material listed above.

Nonmolecular character data from 42 didelphid species (the same terminal taxa sequenced for *Irbp* and *Dmp1*) were extracted from Voss and Jansa (2005:appendix 1) and Voss et al. (2005:appendix 1). Nonmolecular character data from *Chacodelphys formosus* (not represented by *Irbp* or *Dmp1* sequences) were extracted from Voss et al. (2004).

Because the nonmolecular characters defined by Voss and Jansa (2003) were intended to resolve relationships among members of the didelphid subfamily Didelphinae using caluromyines as the designated outgroup, they are not suitable for analyzing relationships among other (nondidelphimorph) marsupials, or among marsupials and placental outgroups. Defining new characters to resolve relationships among nondidelphid terminals is beyond the scope of this report, so the available nonmolecular data play a subsidiary role in the analyses reported below.

Phylogenetic analyses.—We analyzed our molecular data by using maximum-parsimony (MP), maximum-likelihood (ML), and Bayesian methods. Parsimony analyses of molecular sequences were executed by using heuristic search algorithms implemented by PAUP* 4.0b10 (Swofford 2002) with all characters unordered and equally weighted. Parsimony analyses of the nonmolecular data followed the same procedures, with the important exception that some multistate morphological characters were treated as ordered (additive) transformation series for the reasons explained by Voss and Jansa (2003). An initial search for each data set employed 1,000 replicates of random taxon addition and tree-bisection-reconnection (TBR) branch swapping with only 5 trees saved per replicate. The resulting pool of minimal-length trees was then subjected to a 2nd round of TBR branch swapping with no limit on the number of trees saved. Nonparametric bootstrap values (Felsenstein 1985) were computed from heuristic analyses (each with 10 random-addition replicates, TBR branch swapping, and 5 saved trees) of 1,000 pseudoreplicated data matrices.

To implement ML analyses, we examined the relative fit of various models of nucleotide substitution for the *Irbp* and *Dmp1* data separately and in combination by using the Akaike information criterion (AIC) as implemented in Modeltest 3.6 (Posada and Crandall 1998). Log-likelihood scores and estimated parameter values for the various models were calculated based on a neighbor-joining tree of Jukes–Cantor corrected distances. Once the best-fit model of nucleotide substitution was chosen, we used an additional AIC-based

comparison to evaluate whether a molecular clock could be enforced. Subsequent to model evaluation and selection, the ML tree for each gene and for the combined-gene data set was determined by using a heuristic search in which parameter values were initially fixed according to the best-fit model and 10 replicates of random taxon-addition were used as a starting point for TBR branch swapping.

We performed a Bayesian analysis on the combined-gene data set by using MrBayes version 3.01 (Huelsenbeck and Ronquist 2001) running in parallel implementation (Altekar et al. 2004). We allowed all substitution parameters to vary independently between the 2 genes and allowed branch lengths to be estimated proportionally for each gene. We conducted 3 independent runs of Metropolis-coupled Markov chain Monte Carlo (with 4 incrementally heated chains each), in which we specified a model with 6 categories of base substitution, a Γ -distributed rate parameter, and a proportion of invariant sites (GTR+ Γ +I). Uniform-interval priors were assumed for all parameters except base composition, which assumed a Dirichlet prior. The 3 runs were allowed to proceed for 5×10^6 , 2×10^6 , and 2×10^6 generations, respectively, and trees were sampled every 100 generations for each. To ensure that each run converged on the same average log-likelihood, we plotted the log-likelihood values against generation time for each run. In addition, to evaluate whether the 3 independent runs converged on similar nodal posterior probability values, we examined the correlation between nodal posterior estimates derived from each run. We based our final posterior probability estimates on the 1st (longest) run. We discarded the first 500,000 generations (5,000 trees) from this run as burn-in (as determined by plotting log-likelihood scores for each generation and discarding those before the point of stationarity), and calculated estimated parameter values and posterior probabilities for each node based on the remaining trees.

RESULTS

Molecular data characteristics.—The *Irbp* sequences that we obtained from both available tissue samples of *Hyladelphys* are 1,158 bp long, translate to open reading frame, and can be aligned unambiguously with didelphid *Irbp* sequences, all of which are also 1,158 bp in length. By contrast, all of the nondidelphid *Irbp* sequences that we analyzed are shorter than 1,158 bp and include a small region of 35 alignment-ambiguous nucleotide positions corresponding to bp 1,050–1,084 of the human gene; following Jansa and Voss (2000), we coded this alignment-ambiguous region as missing in nondidelphid terminals for the purpose of subsequent phylogenetic analyses.

The *Dmp1* sequence that we obtained from tissue sample T4385 is 1,173 bp long, translates to open reading frame, and can be aligned unambiguously with didelphid *Dmp1* sequences despite modest length variation among the latter (from 1,011 to 1,176 bp; Jansa et al., in press). Although we were unable to obtain the first 597 bp of *Dmp1* sequence from tissue sample TK73757, the remaining 576 bp are unambiguously alignable with the *Dmp1* sequence from T4385 and with the *Dmp1* sequences of didelphids. However, nondidelphid *Dmp1* sequences obtained in our laboratory and others downloaded from GenBank are not unambiguously alignable with those of *Hyladelphys* or with those of didelphids, so the phylogenetic information they might contain is effectively inaccessible for the purpose of this study.

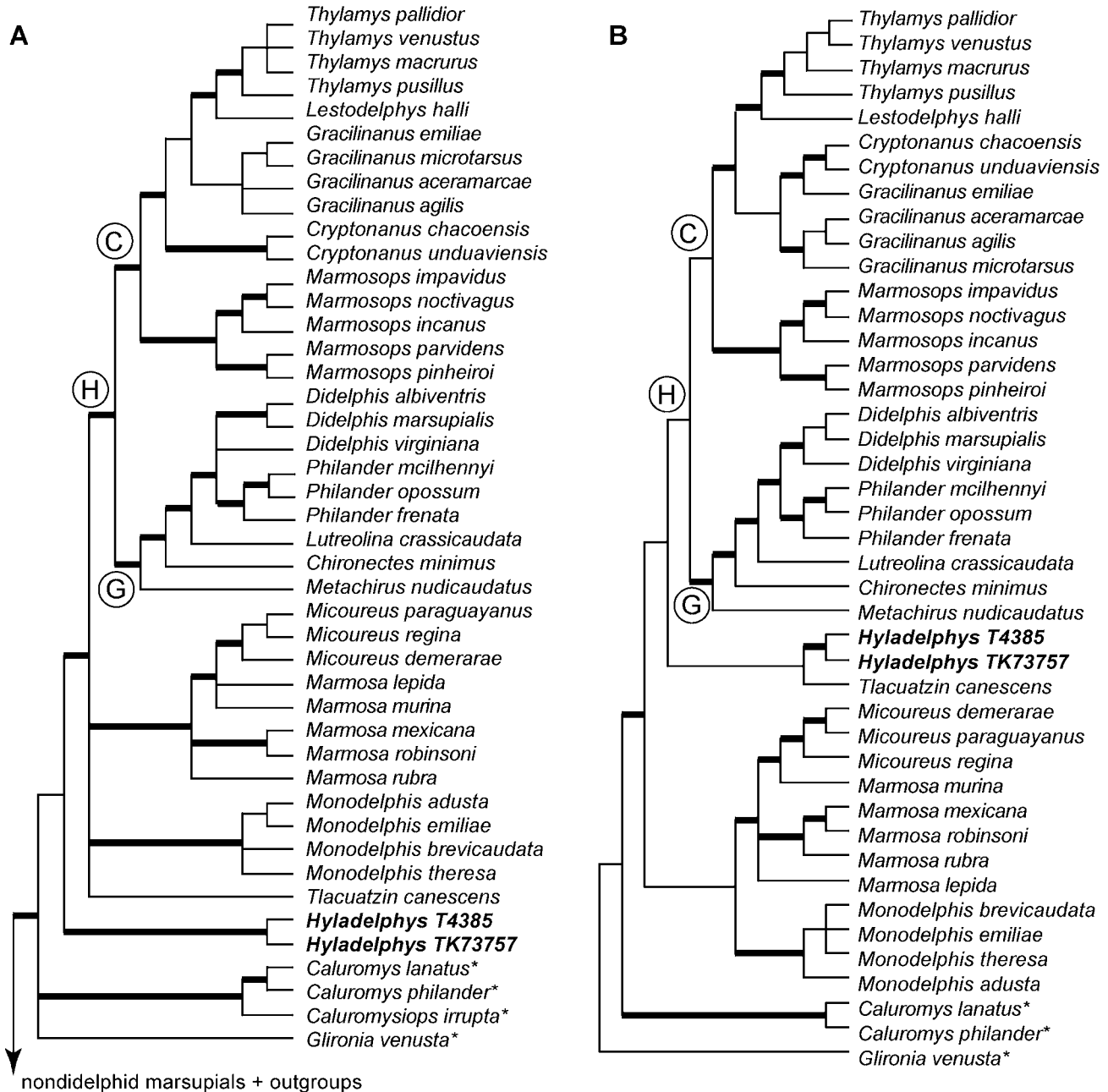


FIG. 1.—Strict consensus trees resulting from parsimony analyses of A) interphotoreceptor retinoid-binding protein gene (*Irbp*) sequence data (550 informative characters, 61 terminal taxa) with placentals as designated outgroups, B) dentin matrix protein 1 gene (*Dmp1*) sequence data (261 informative characters, 43 terminal taxa) rooted at *Glironia*, C) nonmolecular data (67 informative characters, 44 terminal taxa) rooted at *Glironia*, and D) the combined-data matrix (*Irbp* + *Dmp1* + nonmolecular characters for 44 terminal taxa) rooted at *Glironia*. See text for tree lengths and ensemble support statistics. Heavy lines denote branches recovered with $\geq 75\%$ bootstrap support. Asterisks (*) indicate “caluromyine” lineages and alphabetic labels (C, H, G, and J; after Jansa and Voss 2000) identify didelphine clades discussed in the text.

Despite the morphological similarity of examined voucher specimens, the molecular sequences we obtained from T4385 and TK73757 are notably divergent. Whereas conspecific *Irbp* sequences are usually identical or differ by just a few base substitutions (Jansa and Voss, 2000), the *Irbp* sequences from these Peruvian and French Guianan samples differ at 11 sites, a number that is equivalent to an uncorrected divergence value of about 1%. Uncorrected divergence between the *Dmp1* sequences obtained from these samples is even higher (2.4%),

but the range of intraspecific sequence variation among didelphids for this gene is unknown.

Nonmolecular characters.—We were able to score *Hyladelphys* for all of the 67 morphological characters defined by Voss and Jansa (2003), but 4 chromosomal characters were coded as missing in the absence of karyotypic preparations. Our nonmolecular data for *Hyladelphys* are therefore 94% complete. By comparison, didelphid species scored for previous analyses of the same set of nonmolecular characters

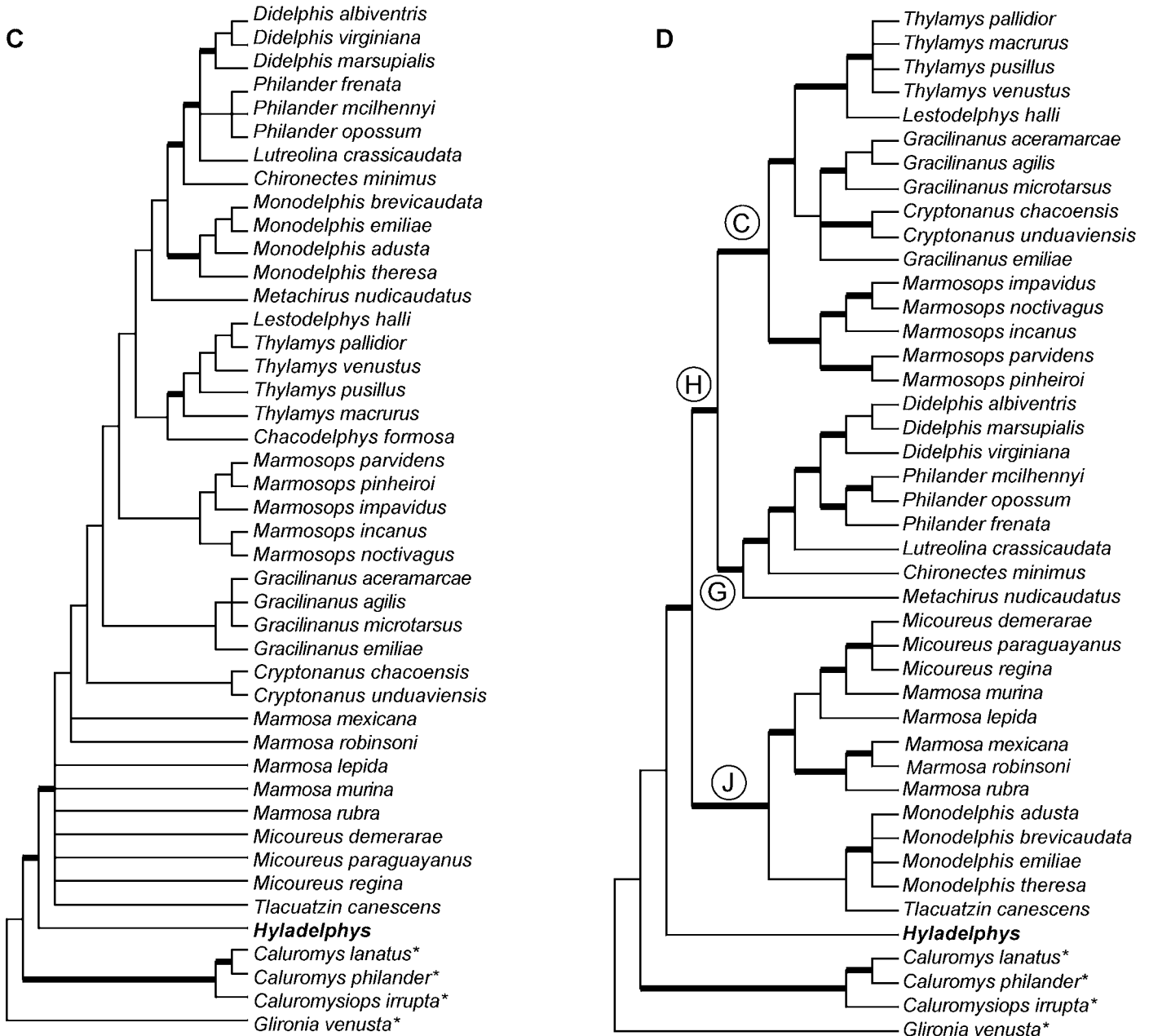


FIG. 1.—Continued.

range from 83% to 100% complete (Voss and Jansa 2003:46, table 3; Voss et al. 2005:22, table 11). The nonmolecular data matrix used for the phylogenetic analyses that follow is reproduced in Appendix I.

Our series of *Hyladelphys* is monomorphic for most anatomical characters, but the number of mental foramina (Voss and Jansa 2003: character 50) exhibits noteworthy polymorphism. Of 5 adult specimens scored bilaterally for this character, 2 (AMNH 267338 and 267003) have 2 mental foramina on each hemimandible, 2 others (FMNH 65754 and 89991) have a single foramen on each hemimandible, and 1 (AMNH 267339) has 2 foramina on the left hemimandible but only 1 foramen on the right hemimandible. A 6th specimen (ROM 34271) has 2 foramina on the left hemimandible (the

right hemimandible is missing). Because both states are present with approximately equal frequency in our material, we treated this polymorphism as an intermediate condition between the 2 fixed states previously recognized by Voss and Jansa (2003), whose coding was modified accordingly.

Parsimony analyses.—Maximum parsimony analysis of the *Irbp* data with placentals as the designated outgroup resulted in 82 equally parsimonious trees (length = 2,271, consistency index [CI] = 0.52, retention index [RI] = 0.72), the strict consensus of which depicts *Hyladelphys* as nested within the family Didelphidae (Fig. 1A). Very strong bootstrap support (100%) for didelphid monophyly provides compelling evidence that *Hyladelphys* belongs in this clade. Among didelphids, the most parsimonious position for *Hyladelphys* is

on the branch that separates the so-called “caluromyine” genera (*Caluromys*, *Caluromysiops*, and *Glironia*) from the subfamily Didelphinae (comprising all other didelphids), and bootstrap support for the nodes that determine this placement is moderately strong: 70% for *Hyladelphys* + Didelphinae and 87% for Didelphinae alone. Despite the relatively high sequence divergence previously noted between samples T4385 and TK73757, these terminals are unambiguously more closely related to one another than they are to any others in our analysis, thus corroborating the status of *Hyladelphys* as a distinct lineage. All of the other illustrated relationships in this topology are the same as those recovered in previous parsimony analyses of didelphid *Irbp* sequences (e.g., Voss et al. 2005).

Because of the absence of alignable *Dmpl* sequences from nondidelphids (see above), parsimony analysis of this gene resulted in 9 undirected networks (length = 792, CI = 0.72, RI = 0.81) that we rooted at *Glironia* to compute a strict consensus topology (Fig. 1B). This tree differs conspicuously from the *Irbp* consensus topology described above because *Hyladelphys* is nested within the subfamily Didelphinae as the sister taxon of *Tlacuatzin canescens*. However, bootstrap support for the nodes that determine this placement is weak: <50% for *Hyladelphys* + *Tlacuatzin* and for *Hyladelphys* + *Tlacuatzin* + clade H. As in the *Irbp* results described above, the 2 tissue samples of *Hyladelphys* cluster together with very strong (100%) bootstrap support despite their substantial sequence divergence. All of the other relationships shown in Fig. 1B are the same as those recovered in previous parsimony analyses of didelphid *Dmpl* sequences (Jansa et al., in press).

Parsimony analysis of both genes combined, with placental *Irbp* sequences as the designated outgroup, recovered 8 minimal-length trees (length = 1,220, CI = 0.70, RI = 0.82) whose strict consensus topology (not shown) closely resembles that obtained by analyzing *Dmpl* separately. However, although bootstrap support for most nodes is substantially higher in the combined-gene parsimony tree than they are in either of the preceding single-gene parsimony analyses, support for *Hyladelphys* + *Tlacuatzin* and *Hyladelphys* + *Tlacuatzin* + clade H remains weak (<50%).

Parsimony analysis of the nonmolecular data resulted in 1,098 undirected networks (length = 177, CI = 0.50, RI = 0.84) that we rooted at *Glironia* to compute a strict consensus topology (Fig. 1C). Although this tree differs in many ways from both the *Irbp* and *Dmpl* topologies, all of the nodes that are strongly supported by nonmolecular characters are also strongly supported by one or the other or both genes. As in previously reported analyses of morphological and molecular data sets (Jansa et al., in press; Voss and Jansa 2003; Voss et al. 2005), there are no examples of “hard” incongruence in these results. Like *Irbp*, morphological characters analyzed with parsimony place *Hyladelphys* on the branch that separates the 3 “caluromyine” genera from the subfamily Didelphinae, and bootstrap support for the nodes that determine this position is moderately strong: 75% for *Hyladelphys* + Didelphinae and 81% for Didelphinae alone. The remaining relationships depicted in this tree are essentially the same as those recovered

in previous parsimony analyses of didelphid nonmolecular data sets (e.g., Voss and Jansa 2003; Voss et al. 2005).

Parsimony analysis of a matrix containing all of the available data (*Irbp* + *Dmpl* + nonmolecular characters), with placentals as the designated outgroup and the 2 *Hyladelphys* sequences combined to form a single terminal, resulted in 24 equally-parsimonious trees (length = 1,397, CI = 0.67, RI = 0.81) whose strict consensus topology (Fig. 1D) closely resembles the *Irbp*-only parsimony topology (Fig. 1A) but is more completely resolved. Again, *Hyladelphys* occupies the branch between “caluromyines” and the subfamily Didelphinae, but bootstrap support for the nodes that determine this position is moderately to very strong: 100% for *Hyladelphys* + Didelphinae and 76% for Didelphinae alone. All of the other clades recovered by this analysis are the same as those obtained in a previous parsimony analysis of didelphid relationships based on both genes plus morphology (Jansa et al., in press).

Likelihood analyses.—The most complex model of nucleotide substitution implemented to date (GTR+I+ Γ , no clock) provides the best fit to the *Irbp* data set according to the AIC. The best tree resulting from a heuristic search under this model (Fig. 2A) supports a monophyletic Didelphidae with *Hyladelphys* as a lineage intermediate between the 3 “caluromyine” genera on the one hand and the subfamily Didelphinae on the other. However, bootstrap support for the nodes that determine this position is only moderate to weak: 77% for *Hyladelphys* + Didelphinae and 57% for Didelphinae alone. Although this topology is similar to that obtained from parsimony analysis of the same data, the sequence of “caluromyine” branching differs; although *Glironia* was the basalmost branch in the parsimony analysis (Fig. 1A), *Caluromys* + *Caluromysiops* is the basalmost branch in this ML analysis. The remaining (didelphine) relationships recovered by this analysis differ from the parsimony results only by resolving the relationships of *T. canescens* as the basalmost member of clade J, albeit with weak (39%) bootstrap support.

The optimal tree resulting from likelihood analysis of *Dmpl* under its best-fit model (GTR+ Γ , no clock; Fig. 2B) differs from the parsimony consensus for the same data (Fig. 1B) by recovering *Hyladelphys* as part of a monophyletic group of higher didelphines. However, bootstrap support for the nodes that determine this position is weak: 40% for *Hyladelphys* + clade C and 53% for *Hyladelphys* + clade C + clade G. Another difference from the parsimony results is the position of *Tlacuatzin* as the sister taxon of *Monodelphis*, but bootstrap support for this result also is weak (34%). In the context of our subsequent discussion, we note that the branches associated with *Hyladelphys* and *Tlacuatzin* in this topology are longer than any others estimated by ML from these *Dmpl* sequence data.

The optimal tree recovered from a likelihood analysis of the combined-gene (*Irbp* + *Dmpl*) data set under its best-fit model (TIM+ Γ +I, no clock) differs from the parsimony consensus for the same data (described but not illustrated above) by placing *Hyladelphys* on the branch between the 3 “caluromyine” genera and the subfamily Didelphinae. Bootstrap support values for the 2 nodes that determine this position are

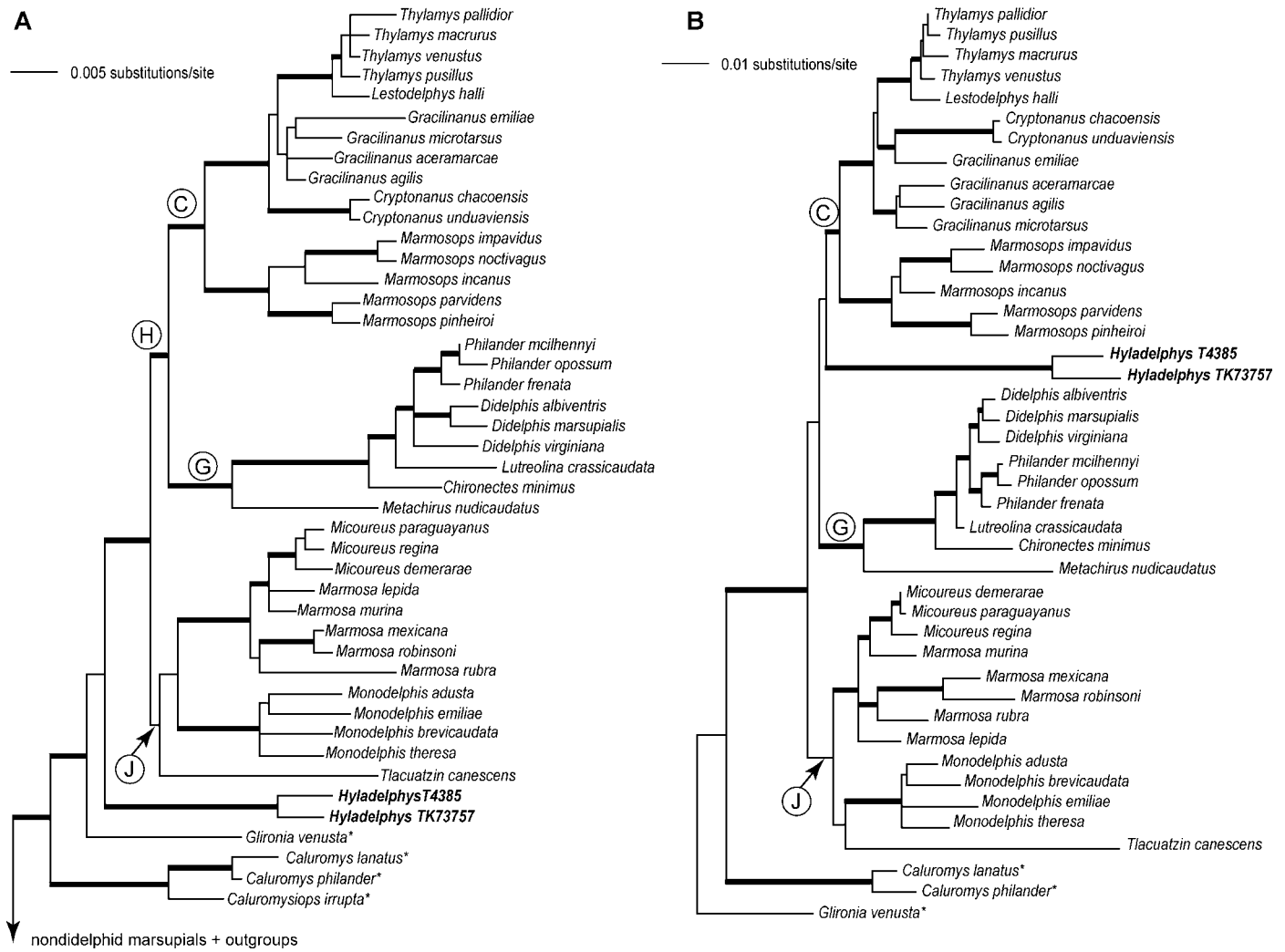


FIG. 2.—Trees resulting from maximum-likelihood analysis of A) the interphotoreceptor retinoid-binding protein gene (*Irpb*) data set under its best-fit model (GTR+I+ Γ ; $r_{AC} = 1.74$, $r_{AG} = 5.44$, $r_{AT} = 1.58$, $r_{CG} = 1.16$, $r_{CT} = 6.50$, $\pi_A = 0.23$, $\pi_C = 0.29$, $\pi_G = 0.28$, $\pi_T = 0.20$, $\alpha = 1.26$, $P_{inv} = 0.25$) with placentals as designated outgroups, and B) the dentin matrix protein 1 gene (*Dmp1*) data set under its best-fit model (GTR+ Γ ; $r_{AC} = 1.13$, $r_{AG} = 2.69$, $r_{AT} = 0.40$, $r_{CG} = 0.77$, $r_{CT} = 6.77$, $\pi_A = 0.37$, $\pi_C = 0.18$, $\pi_G = 0.27$, $\pi_T = 0.18$, $\alpha = 0.69$, $P_{inv} = 0$) rooted on *Glironia*. Heavy lines denote branches recovered with $\geq 75\%$ bootstrap support. Asterisks (*) indicate “caluromyine” lineages and alphabetic labels (C, H, G, and J; after Jansa and Voss 2000) identify didelphine clades discussed in the text.

conspicuously unequal: 99% for *Hyladelphys* + Didelphinae and 44% for Didelphinae alone. The remaining relationships recovered by this analysis are the same as those previously reported by Jansa et al. (in press) for ML analysis of a combined-gene matrix that omitted *Hyladelphys*.

Bayesian analyses.—Because ML analysis of the combined-gene data set under a single model cannot account for gene-specific differences in model parameterization and estimated parameter values, we conducted a Bayesian analysis of the combined-gene data set that allows parameter estimation for *Irpb* and *Dmp1* to be decoupled. In general, estimated posterior probabilities (symbolized by nodal shading in Fig. 3) are similar to corresponding bootstrap values derived from the combined-gene ML analysis: with a single exception, nodes with posterior probability estimates ≥ 0.95 were recovered in $>85\%$ of bootstrap pseudoreplicates. The one exception,

a clade including *Micoureus*, *Marmosa*, *Monodelphis*, and *Tlacuatzin* (clade J) had an estimated posterior probability of 1.0 in the Bayesian analysis, but this node was recovered in only 68% of the bootstrap pseudoreplicates in the combined-gene ML analysis.

DISCUSSION

Higher classification.—Analyses of *Irpb* sequence data using both parsimony and likelihood methods provide strong support for the hypothesis that *Hyladelphys* is a member of the family Didelphidae. Although phylogenetic evidence of familial membership from other data sets is not yet available, the observation that *Dmp1* sequences from *Hyladelphys* can be aligned unambiguously with those of didelphids but not with those of nondidelphid marsupials or placentals is at least consistent with the *Irpb* results. Likewise, although didelphids

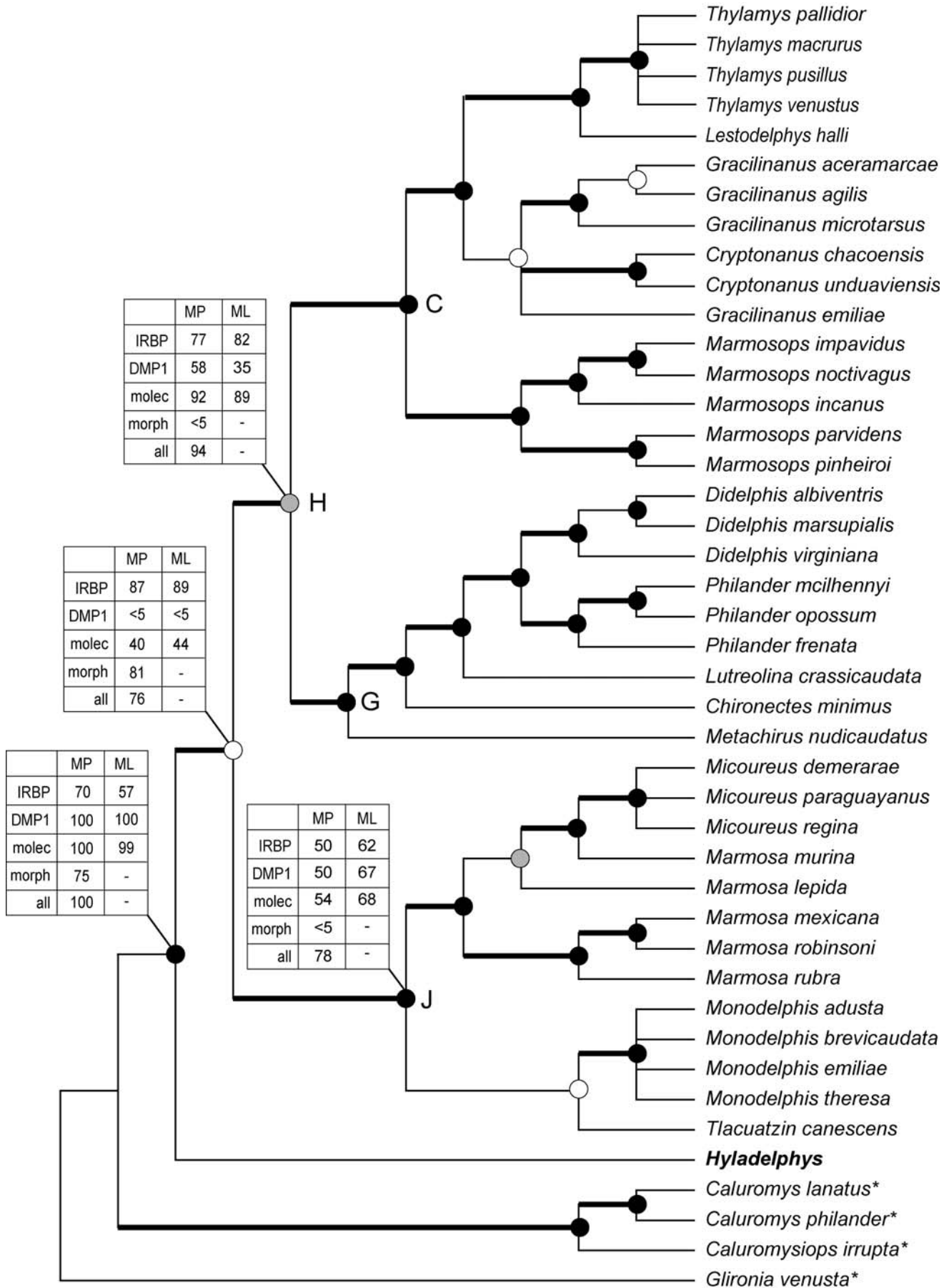


TABLE 1.—Results of phylogenetic analyses based on interphotoreceptor retinoid-binding protein gene (*Irbp*), dentin matrix protein 1 gene (*Dmp1*), and nonmolecular characters.

Data set	Method ^a	Placement of <i>Hyladelphys</i>
<i>Irbp</i>	MP	Between “caluromyines” and Didelphinae
<i>Irbp</i>	ML	Between “caluromyines” and Didelphinae
<i>Dmp1</i>	MP	Nested within Didelphinae, sister group to <i>Tlacuatzin</i>
<i>Dmp1</i>	ML	Nested within Didelphinae, sister group to clade C
<i>Irbp</i> + <i>Dmp1</i>	MP	Nested within Didelphinae, sister group to <i>Tlacuatzin</i>
<i>Irbp</i> + <i>Dmp1</i>	ML	Between “caluromyines” and Didelphinae
<i>Irbp</i> + <i>Dmp1</i>	B	Unresolved trichotomy (posterior probabilities < 0.5) with clades H and J
Nonmolecular	MP	Between “caluromyines” and Didelphinae
All data	MP	Between “caluromyines” and Didelphinae

^a B, Bayesian; ML, maximum likelihood; MP, maximum parsimony.

are difficult to diagnose in terms of derived morphological traits that are preserved in our material (see introduction), *Hyladelphys* is conspicuously unlike members of other marsupial groups in numerous details of integumental, cranial, and dental anatomy. For example, *Hyladelphys* does not exhibit any of the dasyuromorph synapomorphies discussed by Wroe (1997), nor does it share any of the derived conditions hitherto considered to diagnose microbiotherians, paucituberculates, or peramelemorphs. Based on the information at hand, we conclude that *Hyladelphys* is a didelphid and that its previously noted resemblances to certain other marsupials in milk-tooth reduction and mammary counts are plausibly interpreted as convergent.

Relationships within Didelphidae.—Among the 9 analyses that we carried out based on different permutations of data and methods (Table 1), the most consistently supported position for *Hyladelphys* is on the branch that separates basal didelphids (“caluromyines”) from the subfamily Didelphinae. Although nodal support for this placement varies from analysis to analysis and is never consistently strong, no competing hypothesis has anything other than weak support. Also, although character support for the hypothesis that *Hyladelphys* is intermediate to “caluromyines” on the one hand and didelphines on the other comes from both *Irbp* and morphology (Table 2), all of the conflicting indications—that *Hyladelphys* is sister to *Tlacuatzin* or to clade C within Didelphinae—come from *Dmp1*. It is therefore reasonable to consider what properties of the *Dmp1* data might explain such anomalies.

Because *Hyladelphys* and *Tlacuatzin* have the longest estimated branch lengths in the *Dmp1* likelihood topology (Fig. 2B),

TABLE 2.—Morphological traits supporting an intermediate position of *Hyladelphys* between “caluromyines” and Didelphinae.

Characters ^a	“Caluromyines”	<i>Hyladelphys</i>	Didelphinae
Body fur extends onto tail	dorsally > ventrally	dorsally = ventrally*	dorsally = ventrally*
Ventral surface of tail base	with raised tubercles	with smooth scales*	with smooth scales*
Posterior palatal morphology	<i>Caluromys</i> -like	<i>Didelphis</i> -like*	<i>Didelphis</i> -like*
I2–5 crowns	asymmetrical	asymmetrical	rhomboidal*
P3 cutting edges	anterior and posterior	anterior and posterior	posterior only*
Ectoloph	weakly dilambdodont	weakly dilambdodont	strongly dilambdodont*

^a Defined by Voss and Jansa (2003) as follows: body fur extent on tail (character 21), ventral surface of tail base (character 24), posterior palatal morphology (character 42), I2–5 crowns (character 52), P3 cutting edges (character 56), ectoloph (character 58). Asterisks (*) indicate locally derived conditions as reconstructed by parsimony on the topology illustrated in Fig. 3.

we conjectured that these taxa might have been recovered together as a clade in our parsimony analysis of the same data (Fig. 1B) because of long-branch attraction, an often-cited weakness of parsimony analysis (Felsenstein 1978; Huelsenbeck 1995; Swofford et al. 2001). This interpretation appears to be supported by the results of Siddall–Whiting taxon-deletion permutations, which are based on the premise that adjacent long branches in a parsimony tree are unlikely to have attracted one another if removing one and reanalyzing the data leaves the other in the same position (Siddall and Whiting 1999). In the present application of this criterion, deleting *Hyladelphys* and reanalyzing the *Dmp1* matrix by using parsimony resulted in *Tlacuatzin* changing position to join clade J in an unresolved trichotomy with *Monodelphis* and *Marmosa* + *Micoureus*. By contrast, *Hyladelphys* remained as the sister taxon to clade H when *Tlacuatzin* was removed and the data were reanalyzed. Thus, the *Dmp1* sequence from *Tlacuatzin* appears to be attracted to that of *Hyladelphys* (but not vice versa) under parsimony. The fact that these sequences were not recovered as sister taxa in the ML tree is consistent with the relative insensitivity of likelihood to long-branch attraction, and lends credence to our conclusion that the sister-group relationship between *Hyladelphys* and *Tlacuatzin* is an artifact of analysis.

Long-branch attraction in our parsimony analysis of *Dmp1* sequences may be exacerbated by similar base-compositional profiles in these problematic taxa. The *Dmp1* sequences from *Tlacuatzin* and *Hyladelphys* exhibit the highest GC content at 3rd codon positions (GC₃) across all sequenced didelphids (*Hyladelphys* average GC₃ = 45.8%; *Tlacuatzin* GC₃ = 46.2%; other didelphines GC₃ = 38.5–43.6%). Although this dis-

←

FIG. 3.—Summary cladogram (based on parsimony analysis of the combined-data matrix) with nodal support statistics from other analyses superimposed. Heavy lines denote branches recovered with ≥75% bootstrap support based on parsimony analyses of the combined data (interphotoreceptor retinoid-binding protein gene [*Irbp*] + dentin matrix protein 1 gene [*Dmp1*] + nonmolecular characters). Bootstrap support from other parsimony and maximum-likelihood analyses are provided in tabular format. Nodal shading represents posterior probabilities estimated by Bayesian analysis of the combined-gene (*Irbp* + *Dmp1*) data set in which parameter estimation between loci was decoupled: black ≥0.95, gray = 0.5–0.95, white <0.5. Asterisks denote “caluromyine” lineages and alphabetic labels (C, H, G, and J; after Jansa and Voss 2000) identify didelphine clades discussed in the text.

parity in GC₃ values is not statistically significant when base-compositional stationarity is tested across taxa (*Tlacuatzin*: $\chi^2 = 4.81$, $P = 0.19$; *Hyladelphys* T4385: $\chi^2 = 6.05$, $P = 0.11$; *Hyladelphys* TK73757: $\chi^2 = 2.06$, $P = 0.56$), it might be enough to contribute to the results we obtained under parsimony. Why *Hyladelphys* appears as the sister taxon of clade C in our *Dmp1* likelihood consensus topology (Fig. 2B) is less readily explained. However, this relationship was recovered in <50% of our bootstrap pseudoreplicates, and a Shimodaira–Hasegawa test (1,000 RELL replicates, $\delta = 2.90$, $P = 0.205$) based on the *Dmp1* data was unable to reject an alternative tree that placed *Hyladelphys* as intermediate between “caluromyines” and Didelphinae. Although these results suggest that the relationships recovered from other permutations of our data and methods are not strongly contradicted by *Dmp1*, *Hyladelphys* appears to be an exception to the rule that *Irbp* and *Dmp1* generally provide complementary signal in phylogenetic analyses of didelphid sequences (Jansa et al., in press).

Support statistics from all 9 analyses mapped onto the topology obtained from the parsimony analysis of the combined-data matrix (*Irbp* + *Dmp1* + nonmolecular characters) summarize relevant patterns of congruence and conflict in the results at hand (Fig. 3). Despite certain aspects of this synthesis that remain weakly supported, notably by Bayesian posterior probabilities, other details seem sufficiently robust to reject a number of alternative hypotheses. For example, there is clearly no support in these results for a close relationship between *H. kalinowskii* and formerly congeneric species of *Gracilinanus*; instead, the latter are securely nested within clade C along with *Marmosops*, *Thylamys*, *Lestodelphys*, and *Cryptonanus*. Likewise, a close relationship between *Hyladelphys* and *Tlacuatzin* seems implausible based on the very high Bayesian posterior probability estimate for clade J, which convincingly associates *Tlacuatzin* with *Monodelphis* and the *Marmosa* + *Micoureus* complex. Lastly, a sister-group relationship between *Hyladelphys* and clade C is inconsistent with moderately strong support for node H (a diverse cluster of large- and small-bodied didelphines) from several analytic sources.

Strong support from most analyses indicates that *Hyladelphys* shares a more recent common ancestor with didelphines than with any “caluromyine” lineage, but its status as the sister-group of Didelphinae or (alternatively) as a lineage within the didelphine radiation remains to be convincingly established. The absence of Bayesian support for a didelphine clade that excludes *Hyladelphys* is conspicuous despite moderately strong bootstrap support for such a node from analyses that do not include *Dmp1* sequences. Although this issue cannot be resolved convincingly in the absence of additional data, it seems clear that *Hyladelphys* belongs somewhere near the base of the didelphine radiation, where its relatively deep position could significantly affect phenotypic character optimizations in future studies of New World marsupial evolution.

SYSTEMATIC SUMMARY

The diagnosis and description of *Hyladelphys* provided by Voss et al. (2001) included irrelevant information (about traits

common to all didelphid taxa) and omitted many characters that were subsequently found to be taxonomically informative (Voss and Jansa 2003). The following account summarizes relevant morphological information in a more accessible format than the numerical codes used in the appendix, includes additional descriptive details that are helpful for specimen identification, and comments on aspects of species-level diversity that remain to be adequately investigated.

Hyladelphys Voss, Lunde, and Simmons, 2001

Emended morphological description.—Very small didelphid marsupials (for measurements and weight data see Voss et al. 2001:33, table 4) distinguished from other confamilial taxa by the following combination of character states: rhinarium with 2 ventrolateral grooves on both sides of median sulcus; dark circumocular mask present, extending posteriorly from mystacial region to base of ear on each side of face; pale supraocular spot absent; dark midrostral stripe absent; throat gland absent; ears very large (covering eyes when laid forward), membranous, and sparsely haired. Dorsal pelage unpatterned reddish brown with dark gray hair bases; dorsal guard hairs short and inconspicuous; ventral fur self-white. Manus paraxonic (dIII and dIV subequal in length); manual claws relatively large, strongly recurved, and slightly longer than fleshy apical pads; central palmar epithelium more-or-less smooth (not densely tubercular); sexually dimorphic carpal tubercles absent. Pedal digits unwebbed; pedal digit IV longer than adjacent digit III; plantar surface naked from heel to toes. Pouch absent; mammae 2–0–2 = 4, all abdominal–inguinal. Scrotal epithelium (observed in just 1 adult male) blue. Cloaca present (urogenital and rectal openings closely juxtaposed and sharing a common mucosa in both sexes). Tail longer than head-and-body, slender (not incrassate), and apparently naked (without a conspicuously furred base); caudal scales in both annular and spiral series; caudal hairs 3 per scale; central hair of each caudal-scale triplet longer and thicker than the lateral hairs but not grossly petiolate); ventral caudal surface modified for prehension only near tip (not basally).

Premaxillary rostral process absent; palatal process of premaxilla contacts C1 alveolus on each side. Nasals long (extending anteriorly above or beyond I1) and conspicuously widened posteriorly (at or near the maxillary–frontal suture). Maxillary turbinals elaborately branched. Interorbital region strongly convergent anteriorly, with beaded dorsolateral margins; postorbital processes absent. Parietal and alisphenoid in contact on lateral braincase (no frontal–squamosal contact). Petrosal laterally exposed in an open cleft (not a fenestra) between squamosal and parietal. Sagittal crest absent.

Incisive foramina long (extending posteriorly between canines); maxillopalatine fenestrae present but not very wide, long in some specimens (extending from P3 to M3) but discontinuous in others; palatine and maxillary fenestrae absent; posterolateral palatal foramina small, not extending lingual to M4 protocones. Posterior palatal morphology more *Didelphis*-like than *Caluromys*-like (see Voss and Jansa [2003: character 42] for illustrations and definitions of these morphotypes), with moderately well-developed posterolateral

corners, the internal choanae distinctly constricted behind. Maxillary and alisphenoid bones not in contact (widely separated by palatine) on floor of orbit. Transverse canal foramen present. Alisphenoid tympanic wing (alisphenoid bulla) well developed, smoothly globular, and without a well-developed anteromedial process or lamina (secondary foramen ovale absent); ectotympanic suspension direct (from skull); stapes triangular, with large obturator foramen; fenestra cochleae exposed ventrolaterally, not enclosed in a sinus. Paroccipital process of exoccipital small, rounded, and adnate to petrosal. Dorsal margin of foramen magnum bordered by supraoccipital and exoccipitals.

One or 2 mental foramina present on lateral surface of each hemimandible; angular process acute and strongly inflected.

Unworn crowns of I2–I5 asymmetrical (“incisiform”), with much longer anterior than posterior cutting edges and no distinct distostyle on any tooth. Upper canine (C1) without accessory cusps. First upper premolar (P1) smaller than posterior premolars but well formed and nonvestigial. Second upper premolar (P2) much taller than 3rd upper premolar (P3). P3 with both anterior and posterior cutting edges; deciduous precursor (dP3) very small, its occlusal area <10% that of adjacent M1, and nonmolariform (see Voss et al. [2001:37, table 5] for comparative data and character definitions). Upper molars not strongly carnassialized (postmetacrista only slightly longer than postprotocrista), increasing only slightly in width (transverse dimension) from M1 to M3; centrocrista weakly dilambdodont on M1–3; ectoflexus indistinct on M1, shallow on M2, distinct on M3; anterior cingulum complete on M3. Last upper tooth to erupt is P3.

Lower incisors (i1–4) with distinct lingual cuspids; lower canine (c1) a more-or-less erect, simple, recurved-conical tooth (without a posterior heel or accessory cusp). Second lower premolar (p2) taller than 3rd lower premolar (p3); lower milk premolar (dp3) tiny, vestigial, uni- or bicuspid. Hypoconids labially salient on m1–3; hypoconulids twinned with entoconids; entoconids taller than hypoconulids on m1–3; m4 talonid broad and tricuspid.

Included species.—Only the type species, *Hyladelphys kalinowskii*, is currently recognized, but the high level of molecular divergence reported above between samples from French Guiana and Peru suggests that other species remain to be described. Although Voss et al. (2001) emphasized the morphological similarity of their French Guianan and Peruvian material, we note that both of the adult Peruvian specimens examined for this study have 1 mental foramen on each hemimandible, whereas most French Guianan specimens have 2 foramina on each hemimandible. Although this variation, coded as an intraspecific polymorphism in our phylogenetic analysis, might represent a difference between 2 morphologically cryptic species, adult phenotypes cannot yet be associated with molecular divergence because the adult Peruvian specimens were collected south of the Amazon, whereas the Peruvian tissue sample (from a juvenile individual) was collected north of the Amazon. Potentially, as many as 3 species might be represented in this material (1 each in northeastern, northwestern, and southwestern Amazonia), but more material is clearly needed before any taxonomic changes can be made.

ACKNOWLEDGMENTS

For crucial loans of tissues we thank Chris Hice and François Catzeflis, without whose professional generosity our analyses would have been impossible. We are also grateful to Diego Astúa de Moraes (who imaged the morphology of P3 on MN 20918) and Bruce Patterson (who checked our scoring of mental foramina on FMNH material) for their helpful contributions of time and effort to this project. The Minnesota Supercomputing Institute provided valuable computing resources that facilitated our data analyses. This research was partially supported by a grant from the National Science Foundation (DEB-0211952) and supplementary funding from the University of Minnesota and the American Museum of Natural History.

LITERATURE CITED

- ALTEKAR, G., S. DWARKADAS, J. P. HUELSENBECK, AND F. RONQUIST. 2004. Parallel metropolis-coupled Markov chain Monte Carlo for Bayesian phylogenetic inference. *Bioinformatics* 20:407–415.
- ARCHER, M. 1976. The dasyurid dentition and its relationship to that of didelphids, thylacinids, borhyaenids (Marsupicarnivora), and peramelids (Peramelina: Marsupialia). *Australian Journal of Zoology Supplementary Series* 39:1–34.
- BRESSLAU, E. 1920. The mammary apparatus of the Mammalia in the light of ontogenesis and phylogenesis. Methuen, London, United Kingdom.
- DE MORAES, D. A. In press. Range extension and first record for Brazil of the rare *Hyladelphys kalinowskii* (Hershkovitz, 1992) (Didelphimorphia, Didelphidae). *Mammalia*.
- FELSENSTEIN, J. 1978. Cases in which parsimony and compatibility methods will be positively misleading. *Systematic Zoology* 27: 401–410.
- FELSENSTEIN, J. 1985. Confidence limits on phylogenies: an approach using the bootstrap. *Evolution* 39:783–791.
- GARDNER, A. L., AND G. K. CREIGHTON. 1989. A new generic name for Tate's *microtarsus* group of South American mouse opossums (Marsupialia: Didelphidae). *Proceedings of the Biological Society of Washington* 102:3–7.
- HERSHKOVITZ, P. 1992. The South American gracile mouse opossums, genus *Gracilinanus* Gardner and Creighton, 1989 (Marmosidae, Marsupialia): a taxonomic review with notes on general morphology and relationships. *Fieldiana: Zoology (New Series)* 39:i–vi,1–56.
- HICE, C. L. 2001. Records of a few rare mammals from northeastern Peru. *Mammalian Biology* 66:317–319.
- HUELSENBECK, J. 1995. Performance of phylogenetic methods in simulation. *Systematic Biology* 44:17–48.
- HUELSENBECK, J. P., AND F. RONQUIST. 2001. MrBayes: Bayesian inference of phylogeny. *Bioinformatics* 17:754–755.
- JANSA, S. A., J. F. FORSMAN, AND R. S. VOSS. In press. Different patterns of selection on nuclear genes *Irbp* and *Dmp1* affect the efficiency but not the outcome of phylogeny estimation for didelphid marsupials. *Molecular Phylogenetics and Evolution*.
- JANSA, S. A., AND R. S. VOSS. 2000. Phylogenetic studies on didelphid marsupials I. Introduction and preliminary results from nuclear *Irbp* gene sequences. *Journal of Mammalian Evolution* 7:43–77.
- JANSA, S. A., AND M. WEKSLER. 2004. Phylogeny of muroid rodents: relationships within and among major lineages as determined by *Irbp* gene sequences. *Molecular Phylogenetics and Evolution* 31: 256–276.
- KIRSCH, J. A. W., AND M. ARCHER. 1982. Polythetic cladistics, or, when parsimony's not enough: the relationships of carnivorous marsupials. Pp. 595–620 in *Carnivorous marsupials* (M. Archer,

- ed.). Vol. 2. Royal Society of New South Wales, Mosman, New South Wales, Australia.
- KIRSCH, J. A. W., F.-J. LAPOINTE, AND M. S. SPRINGER. 1997. DNA-hybridization studies of marsupials and their implications for metatherian classification. *Australian Journal of Zoology* 45: 211–280.
- KRAJEWSKI, C., G. R. MOYER, J. T. SAPIORSKI, M. G. FAIN, AND M. WESTERMAN. 2004. Molecular systematics of the enigmatic 'phascosoricine' marsupials of New Guinea. *Australian Journal of Zoology* 52:389–415.
- LUCKETT, W. P., AND N. HONG. 2000. Ontogenetic evidence for dental homologies and premolar replacement in fossil and extant caenolestids (Marsupialia). *Journal of Mammalian Evolution* 7:109–127.
- POSADA, D., AND K. A. CRANDALL. 1998. Modeltest: testing the model of DNA substitution. *Bioinformatics* 14:817–818.
- SIDDALL, M. E., AND M. F. WHITING. 1999. Long-branch abstractions. *Cladistics* 15:9–24.
- SOLARI, S., ET AL. 2001. The small mammals of the lower Urubamba region, Peru. Pp. 171–181 in *Urubamba: the biodiversity of a Peruvian rainforest* (A. Alonso, F. Dallmeier, and P. Campbell, eds.). Smithsonian Institution Press, Washington, D.C.
- SPRINGER, M. S., A. BURK, J. R. KAVANAGH, V. G. WADDELL, AND M. J. STANHOPE. 1997. The interphotoreceptor retinoid binding protein gene in therian mammals: implications for higher-level relationships and evidence for loss of function in the marsupial mole. *Proceedings of the National Academy of Sciences* 94: 13754–13759.
- STANHOPE, M. J., M. R. SMITH, V. G. WADDELL, C. A. PORTER, M. S. SHIVJI, AND M. GOODMAN. 1996. Mammalian evolution and the interphotoreceptor retinoid binding protein (*Irbp*) gene: convincing evidence for several superordinal clades. *Journal of Molecular Evolution* 43:83–92.
- SWOFFORD, D. L. 2002. PAUP*. Phylogenetic analysis using parsimony (*and other methods), version 4. Sinauer Associates, Sunderland, Massachusetts.
- SWOFFORD, D. L., P. J. WADDELL, J. P. HUELSENBECK, P. G. FOSTER, P. O. LEWIS, AND J. S. ROGERS. 2001. Bias in phylogenetic estimation and its relevance to the choice between parsimony and likelihood methods. *Systematic Biology* 50:525–539.
- TEMPLE-SMITH, P. 1987. Sperm structure and marsupial phylogeny. Pp. 171–193 in *Possums and opossums: studies in evolution* (M. Archer (ed.). Surrey Beatty & Sons, Chipping Norton, New South Wales, Australia.
- THOMAS, O. 1888. Catalogue of the Marsupialia and Monotremata in the collection of the British Museum (Natural History). Trustees of the British Museum (Natural History), London, England.
- TOYOSAWA, S., C. O'HUIGIN, AND J. KLEIN. 1999. The dentin matrix protein 1 gene of prototherian and metatherian mammals. *Journal of Molecular Evolution* 48:160–167.
- VOSS, R. A., A. L. GARDNER, AND S. A. JANSA. 2004. On the relationships of "*Marmosa*" *formosa* Shamel, 1930 (Marsupialia: Didelphidae), a phylogenetic puzzle from the Chaco of northern Argentina. *American Museum Novitates* 3442:1–18.
- VOSS, R. S., AND S. A. JANSA. 2003. Phylogenetic studies on didelphid marsupials II. Nonmolecular data and new *Irbp* sequences: separate and combined analyses of didelphine relationships with denser taxon sampling. *Bulletin of the American Museum of Natural History* 276:1–82.
- VOSS, R. S., D. P. LUNDE, AND S. A. JANSA. 2005. On the contents of *Gracilinanus* Gardner and Creighton, 1989, with the description of a previously unrecognized clade of small didelphid marsupials. *American Museum Novitates*. 3482:1–34.
- VOSS, R. S., D. P. LUNDE, AND N. B. SIMMONS. 2001. The mammals of Paracou, French Guiana: a neotropical rainforest fauna. Part 1. Nonvolant species. *Bulletin of the American Museum of Natural History* 263:1–236.
- WEKSLER, M. 2003. Phylogeny of neotropical oryzomyine rodents (Muridae: Sigmodontinae) based on the nuclear *Irbp* exon. *Molecular Phylogenetics and Evolution* 29:331–349.
- WROE, S. 1997. A reexamination of proposed morphology-based synapomorphies for the families of Dasyuromorphia (Marsupialia). I. Dasyuridae. *Journal of Mammalian Evolution* 4:19–52.
- WROE, S., M. EBACH, S. AHYONG, C. DE MUIZON, AND J. MUIRHEAD. 2000. Cladistic analysis of dasyuromorphian (Marsupialia) phylogeny using cranial and dental characters. *Journal of Mammalogy* 81:1008–1024.

Submitted 3 June 2005. Accepted 27 June 2005.

Associate Editor was *Enriques P. Lessa*.

APPENDIX I

The matrix of nonmolecular (morphological and karyotypic) characters analyzed in this report is reproduced below. Character descriptions are given in Voss and Jansa (2003), and an electronic version of the same data in Nexus format can be downloaded from <ftp://ftp.amnh.org/pub/mammalogy>.

Caluromys lanatus: 01100 00002 00020 01100 00211 00011 00010 00000 00000 11000 11010 00100 00000 00000 0
Caluromys philander: 01100 00002 00020 01000 10201 00011 00010 00000 00000 11000 11010 00100 00000 00000 0
Caluromysiops irrupta: 000–0 02002 00020 01700 00211 00001 00011 00000 00002 11000 11010 00000 00000 017?? ?
Chacodelphys formosa: ?0100 10000 1??20 0???? 20000 00000 00100 02211 01010 00000 00000 11211 ?0?21 10??? ?
Chironectes minimus: 10120 01000 20021 01201 11200 00000 01021 00200 01012 10101 00002 11111 21000 00111 1
Cryptonanus chacoensis: 00100 10001 01020 00–00 20001 00000 00000 02210 01010 00000 00102 11211 00000 00??? ?
Cryptonanus unduaviensis: 00100 10001 01020 0???0 20001 00000 00000 02210 01010 00000 00202 11210 00020 00??? ?
Didelphis albiventris: 10100 00110 00010 01100 11201 00000 01021 00210 01012 10110 01002 11111 21000 00111 1
Didelphis marsupialis: 10100 00110 00020 01100 11201 00000 01021 00210 01012 10110 01002 11111 21000 00111 1
Didelphis virginiana: 10100 00110 00010 01100 11201 00000 01021 00210 01012 10110 01002 11111 21000 00111 1
Glironia venusta: 00100 ?0001 0??20 00–00 00–11 ?0000 00010 00100 00010 00000 01001 01110 000?0 00??? ?
Gracilinanus aceramarcae: 00100 10001 01020 00–00 20001 00010 00000 02211 01011 00000 00001 11210 ?00?0 00??? ?
Gracilinanus agilis: 00100 10001 01020 0???0 20001 00010 00000 02211 01011 00000 00001 11210 ?0020 00000 0
Gracilinanus emiliae: 00100 10001 01020 00–00 20101 00010 00000 02211 01011 00000 00101 11210 00020 00??? ?
Gracilinanus microtarsus: 00100 10001 01020 0???0 20001 00010 00010 02211 01011 00000 00001 11210 000?0 00000 0
Hyladelphys kalinowskii: 00100 00001 00020 00–00 20101 00000 00000 00100 01010 00001 01000 01110 00020 00??? ?
Lestodelphys halli: 10100 16000 10000 10–10 20000 ?0100 00000 01210 11011 01000 00002 11211 00221 00000 0
Lutreolina crassicaudata: 100–0 00000 00000 01200 11200 10000 01021 00210 01212 10110 01002 11111 21000 00111 1

Marmosa lepida: 00100 00001 01020 00-00 20201 00010 00010
00200 01010 00000 00101 11210 00020 00??? ?

Marmosa mexicana: 00100 10001 01120 00-00 20101 00010
00010 00210 01010 00000 00001 11210 00020 00000 0

Marmosa murina: 00100 00001 00020 00-00 20201 00010
00010 00200 01010 00000 00001 11210 00020 00000 0

Marmosa robinsoni: 00100 10001 01120 00-00 20101 00010
00010 00200 01010 00000 00001 11210 00020 00000 0

Marmosa rubra: ?0100 00001 01120 00-0? 20201 00010 00000
00200 01010 01000 00001 11210 00020 00??? ?

Marmosops impavidus: 00100 00000 01020 00-00 20201 01010
00000 02210 01011 00000 00001 11211 00000 00000 0

Marmosops incanus: 00100 10000 01020 00-10 20201 010?0
00100 01210 01011 00000 00001 11211 000?0 00000 0

Marmosops noctivagus: 00100 10000 01020 00-00 20201 01010
00000 01210 01011 00000 00001 11211 00000 00000 0

Marmosops parvidens: 00100 00000 01020 00-00 20201 01010
00000 02200 01011 00000 00201 11210 00000 00??? ?

Marmosops pinheiroi: 00100 00000 01020 00-00 20201 01010
00000 02200 01011 00000 00201 11211 00000 00??? ?

Metachirus nudicaudatus: 10121 10000 00020 00-00 20100
00000 00000 10200 01011 00110 00001 11211 10000 00000 0

Micoureus demerarae: 00100 00001 01120 00-00 20201 00010
00010 00200 01010 00000 00001 11210 00020 00000 0

Micoureus paraguayanus: 00100 00001 01120 00-?0 10201
00010 00010 00200 01010 00000 00001 11210 ?00?0 00000 0

Micoureus regina: 00100 00001 01120 00-00 20201 00010
00010 00200 01010 00000 00001 11210 00020 00000 0

Monodelphis adusta: 100-0 10000 00000 00-00 20000 00000
10000 00200 01210 00000 00002 11211 001?1 10??? ?

Monodelphis brevicaudata: 100-0 14000 00000 00-00 00000
00000 10000 00200 01210 00000 00002 11211 10101 10010 1

Monodelphis emiliae: 100-0 15000 00000 00-00 00000 00000
10000 00200 01210 01000 00002 11211 ?0201 10010 1

Monodelphis theresa: 100-0 03000 00000 0???0 20000 00000
10000 00200 01212 00000 00002 11211 ?01?1 10??? ?

Philander frenata: 10111 00000 00020 01100 11201 10000
01021 00210 01012 10110 01002 11111 ?10?0 00111 1

Philander mcilhennyi: 10121 00000 00020 01100 11201 10000
01021 00210 01012 10110 01002 11111 21000 00111 1

Philander opossum: 10121 00000 00020 01100 11201 10000
01021 00210 01012 10110 01002 11111 21000 00111 1

Thylamys macrurus: 00100 16000 10020 10-10 20001 00000
00100 02211 01011 01000 00002 11211 001?0 00000 0

Thylamys pallidior: 10100 16000 10020 1???0 20001 00100
00100 02210 11011 01000 00002 11211 00120 00000 0

Thylamys pusillus: 00100 16000 10020 10-10 20001 00100
00100 02211 11011 01000 00002 11211 00110 00000 0

Thylamys venustus: 00100 16000 10020 1???0 20001 00100
00100 02211 11011 01000 00002 11211 00120 00000 0

Tlacuatzin canescens: 00100 00001 01020 00-00 20001 00000
00010 00201 01010 00000 00001 11210 00020 00111 1